Three-dimensional Analysis of the Intrinsic Anatomy of the Metatarsal Bones

Arnaud Largey, MD,[1] François Bonnel, MD,[2] François Canovas, MD, PhD,[3] Gérard Subsol, PhD,[4] Stéphane Chemouny, PhD,[5] and Frédéric Banegas, PhD[6]

Knowledge of the anatomy of the forefoot is important for understanding its mechanical pathology and developing specific surgical procedures. The aim of this study was to quantify 3-dimensional morphological parameters, which were proposed for the characterization of the metatarsal intrinsic anatomy. Thirty-five metatarsal bones prepared from 7 cadaver specimens were analyzed according to a new 3-dimensional computer-aided (CA) methodology. Manual and CA measurement techniques were compared. The reality of an intrinsic axial torsion of the metatarsals was underlined with mean values between 3.2° and 57.7°. Using the CA method, the reliability was excellent (intraclass correlation coefficient, 0.98) and significantly better than the manual method ($P < .1E\text{-}12$*). With specific consideration of the second metatarsal intrinsic morphology, we emphasized its mechanical function. These results reflect the possibilities of CA systems. These data, which were carried out on specific anatomical characteristics of the metatarsal bones, can improve the metatarsalgia surgical procedures.* (The Journal of Foot & Ankle Surgery 46(6):434–441, 2007)

Key words: human forefoot, computer-assisted image processing, cross-sectional anatomy, 3-dimensional image, medical imaging

Knowledge of foot anatomy is the first step toward understanding mechanical pathology. Nevertheless, 2-dimensional imaging methods such as standard x-rays are not sufficient enough for anatomic study because of a high variability in the observer measurement (1) and in the description of the morphological parameters (2). The development of medical imaging allows the study of 3-dimensional bone anatomy and motion (3, 4). A 3-dimensional imaging process (magnetic resonance imaging [MRI] or computed tomography [CT] scan) and computer-aided (CA) analysis have been associated with measuring wrist or foot biometry and motion (5–10). The results lead to a better modelling of these complex structures with a particular objective in motion characterization. One can visualize the motion of the adult hindfoot bones during ankle plantarflexion (11) or appreciate the subtalar motion with ligament damage in the ankle (12).

Various methods have been reported for analysis of the intrinsic anatomy of bones (13–18). These studies had a specific object and used specially developed techniques. The finite element method has been suggested for a bone modelization and an indirect evaluation of osseous stresses and distortions (13–16). The metatarsal osseous structure has been specified with a densitometric technique (17) or a bidimensional tomodensitometric technique (18).

The aim of this study was to first assess the intrinsic torsion of the metatarsals. In our knowledge, no past studies analyzed this anatomical parameter. We defined this intrinsic torsion as the axial intraosseous rotation between the proximal and distal extremities of a metatarsal bone. For us, this parameter is important for a better understanding of forefoot mechanical problems and evaluation of surgical techniques.

Methods

Cadaver Specimens

The metatarsal bones of 7 feet were studied (2 right and 5 left). The bones were prepared from embalmed cadaver subjects selected from a sample of cadavers available for dissection in a medical anatomy laboratory (subjects of both sexes; age was between 75 and 85 years). The feet had no evidence of local pathology or prior surgery. All soft tissues, except cartilage, were removed from the metatarsal bones.

Address correspondence to: Arnaud Largey, MD, Service Orthopédie 3, Hôpital Lapeyronie, Montpellier CHRU, 371 avenue du Doyen Giraud, 34295, Montpellier cedex 5, France. E-mail: arnaudlargey@hotmail.com.
[1]Foot and Ankle Surgeon, Service Orthopédie 3, Hôpital Lapeyronie, Montpellier, France.
[2]Foot and Ankle Surgeon, Service Orthopédie 3, Hôpital Lapeyronie, Montpellier, France.
[3]Foot and Ankle Surgeon, Service Orthopédie 3, Hôpital Lapeyronie, Montpellier, France.
[4]Senior Scientist, Intrasense SAS, Montpellier, France.
[5]Chairman, Intrasense SAS, Montpellier, France.
[6]Chief Technical Officer, Intrasense SAS, Montpellier, France.
No benefits or funds were received in support of this study.

1067-2516/07/4606-0005$32.00/0
doi:10.1053/j.jfas.2007.08.003

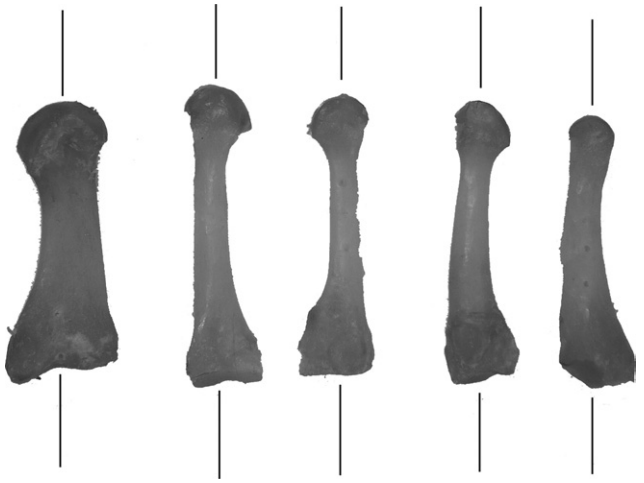

FIGURE 1 Metatarsal set. This was fixed on an x-ray–transparent support with a global alignment by the bones' longitudinal axis.

Manual Biometry

For each metatarsal bone, we measured the length, the cross-sectional diameters, and the intrinsic axial torsion. We used a calliper (graduation to 0.5 mm) for length and diameter measurements. The length was obtained between the supposed centers of the proximal and distal articular areas. The cross-sectional diameters were evaluated on the dorsal and lateral sides of the bone at 3 different levels (basis, midlength diaphysis, head). For the torsion measurement, we used pins to mark the principal axis of the proximal and distal extremities. These axes were chosen by subjective visual considerations. The angle between the 2 pins was read directly by a goniometer (graduation to 1°).

Computer-aided Biometry

A CT scan (LightSpeed 16; General Electric, Milwaukee, WI) was performed on the whole length of each individual set of bones (kV 120; mA 100; 0.62 mm slice thickness; pixel size between 0.29 × 0.29 and 0.45 × 0.45 mm). Each set was composed of the 5 ordered metatarsals. They were fixed parallel on their longitudinal axis on a radiotransparent flat support (Figure 1). The transverse plane of the scan slices was chosen perpendicular to the bones' longitudinal axes. We transferred the collected CT scan data in DICOM format to the MYRIAN (Intrasense SAS, Montpellier, France) image analysis console. This software allowed us to perform a tridimensional and quantitative approach of the metatarsal volumes with precise measurement of some morphological parameters. We have treated the morphological collected data with SCILAB (INRIA–ENPC, LeChesnay, France) programming to obtain final results.

MYRIAN Analysis

The XP-Ortho module of MYRIAN software allowed us to automatically delineate the different metatarsal bones. We used the "edition tools" to define the specific 3-dimensional regions of interest (ROI) (Figure 2). For each metatarsal, we delineated 3 ROIs that represented the 3 bone levels: proximal ROI, midlength ROI, and distal ROI. The distal ROI consisted of the 10 proximal cross slices beginning at 4 mm of distal bone extremity. The proximal ROI consisted of the 10 distal cross slices after the first transversal slice with the entire cortical outline of metatarsal base. The thickness of these 2 extremities' ROI was 4 mm. We defined the midlength ROI by selecting the 5 cross slices (2 mm thickness), which were equidistant to both extreme ROIs. For each ROI, the MYRIAN software automatically computed some tridimensional geometric parameters: the volume (in cm^3), the coordinates of geometric centroid (in mm, according to the 3-dimensional frame of the CT image), the magnitude of the 3 principal moments of inertia (in mm^4), and the coordinates of the 3 principal unit vectors of inertia (in mm, according to the 3-dimensional frame of the CT image).

SCILAB Analysis

These morphometrical parameters were used to compute the intrinsic torsion angles with specific SCILAB programming. The primary principal axis of inertia was considered as the ROI geometric axis, and its corresponding principal vector was used for the angle calculation. An exception in the choice criterion of principal axis was necessary for first metatarsal distal ROI. In this case, we had to choose the principal axis of inertia that was perpendicular to the plantar articular surface of the first metatarsal head. This specific criterion was required because of the quasicircular form of the cross-sectional area of the first metatarsal head that prevents it from having stable axes of inertia. Then, we performed a projection of the selected principal axis vector of each extremity ROI on the cross-sectional plan for specific axial rotation.

The metatarsal intrinsic torsions were the calculated angles between the principal axes' projections of the proximal and distal ROIs. A positive sign was given for axial torsion in pronation and a negative sign for supination. We also noted the 3 levels of cross-sectional volumes and calculated the 3 mean cross-sectional areas for each metatarsal.

Statistical Analysis

The statistical analysis was first a global description of each considered quantitative variable with the calculation of means, standard deviations, median, and interquartiles 25%

TABLE 1 Average results of cross-sectional metatarsal diameters

	M1	M2	M3	M4	M5
Cephalic diameter					
Dorsal view	20.43 ± 2.15	10.43 ± 0.79	8.83 ± 0.98	9.00 ± 1.00	9.00 ± 1.10
Lateral view	20.29 ± 2.50	14.57 ± 1.90	13.33 ± 2.50	14.00 ± 1.63	12.00 ± 1.26
Diaphysis diameter					
Dorsal view	11.29 ± 2.14	6.57 ± 0.79	6.86 ± 1.07	7.29 ± 0.95	9.83 ± 1.17
Lateral view	13.29 ± 1.80	8.57 ± 1.27	8.29 ± 1.70	8.71 ± 1.38	7.33 ± 1.03
Basis diameter					
Dorsal view	17.14 ± 3.02	15.90 ± 1.15	12.86 ± 1.21	15.00 ± 1.53	20.33 ± 1.75
Lateral view	27.71 ± 2.21	18.14 ± 1.95	17.71 ± 1.89	15.71 ± 2.43	12.67 ± 1.21

All values are expressed in mm.

TABLE 2 Results of metatarsal intrinsic torsion with the manual technique

	Foot 1	Foot 2	Foot 3	Foot 4	Foot 5	Foot 6	Foot 7	Means
M1	6	22	17	4	8	18	16	13 ± 6.9
M2	23	0	14	20	4	17	19	14 ± 8.6
M3	57	18	26	29	27	15	32	29 ± 13.7
M4	76	32	20	42	35	30	32	38 ± 17.9
M5	−58	−32	−52	−79	−12	*	−42	−46 ± 23.0

All values are expressed in degrees. They correspond to the first set of measurements. Positive values express a medial axial rotation (pronation) and negative values a lateral axial rotation (supination).
*Not measurable.

to 75%. We used the Shapiro-Wilk test for evaluating the standard distribution of the parameters.

We wanted to appreciate the repeatability in the measurement of the biometric parameters and the potential difference between manual technique and CA technique. For each bone, each of 2 techniques was used 3 times by a unique observer.

For manual measurement, the observer performed metatarsal biometry without knowing the reference number of the bone. During this blind analysis, each metatarsal was presented 3 times without any specific order. Total length and intrinsic torsion were evaluated. The measurement results were collected by an independent observer.

For CA measurement, it was clearly impossible for the observer to know which foot was analyzed. Nevertheless, the MYRIAN software process does not give biometric parameters directly. Therefore, the unique observer repeated the 3 segmentations of the 35 bones without specific order. Each set of results was collected by a different observer. The CA data were analyzed by SciLab processing. Three series of intrinsic torsions and cross-sectional area values were obtained by the CA method. Intraclass correlation coefficients (ICCs) and their confidence interval at 95% were calculated to assess the reliability of measurement repetition.

For intrinsic torsion, the ICCs of the 2 measurement techniques were compared by using a specific calculation for the likelihood ratio test (19).

All the statistical parameters were obtained and analyzed with SAS 9.1.3 software (SAS Institute, Inc., Cary, NC). The results were considered significant for P values less than 5%.

Results

The conservative aspect of bones was excellent. Nevertheless, the cephalic part of the fifth metatarsal of the sixth foot presented an osseous defect. This bone was excluded from our study. The parameters we used for the repeatability analysis are the presented results from the first set of measures.

Manual Biometry

The mean length of the metatarsal bones was 59 ± 4.34 mm for the first metatarsal (M1), 70 ± 6.28 mm for the second (M2), 65 ± 4.07 mm for the third (M3), 65 ± 4.73 mm for the fourth (M4), and 61 ± 2.66 mm for the fifth (M5). The results of the cross-sectional diameters are shown in Table 1. The results of the intrinsic torsion are shown in Table 2.

Computed Data

Intrinsic Torsion The results are shown in Table 3.

Regions of Interest Volumes The average volume of the distal ROI was 0.99 ± 0.19 cm^3 (0.62; 1.19) for M1 and

TABLE 3 Results of metatarsal intrinsic torsion with the CA technique

	Foot 1	Foot 2	Foot 3	Foot 4	Foot 5	Foot 6	Foot 7	Means
M1	13.82	15.06	30.27	43.57	43.89	15.02	2.37	23.43 ± 16.06
M2	2.93	3.48	2.35	3.50	8.73	1.69	0.00	3.24 ± 2.71
M3	39.29	14.88	23.96	33.75	28.03	15.24	25.40	25.79 ± 8.99
M4	45.87	37.32	31.58	45.31	30.76	21.47	22.75	33.58 ± 9.82
M5	−51.64	−57.70	−50.94	−61.01	40.41	*	−85.06	−57.69 ± 15.11

All values are expressed in degrees. They correspond to the first set of measurements. Positive values express a medial axial rotation (pronation) and negative values a lateral axial rotation (supination).
*Not measurable.

TABLE 4 Volumes and ratios results

	Foot 1	Foot 2	Foot 3	Foot 4	Foot 5	Foot 6	Foot 7	Means
Dist. ROI volume								
M1	1.01	1.00	1.15	0.62	0.90	1.07	1.19	0.99 ± 0.19
M2	0.39	0.39	0.50	0.27	0.39	0.40	0.57	0.41 ± 0.09
M3	0.30	0.32	0.37	0.23	0.16	0.16	0.46	0.29 ± 0.11
M4	0.35	0.31	0.38	0.20	0.35	0.33	0.36	0.32 ± 0.06
M5	0.27	0.23	0.27	0.25	0.20	*	0.35	0.26 ± 0.05
Midl. ROI volume								
M1	0.23	0.26	0.27	0.12	0.18	0.18	0.33	0.22 ± 0.07
M2	0.07	0.12	0.08	0.07	0.07	0.08	0.11	0.08 ± 0.02
M3	0.08	0.12	0.09	0.06	0.07	0.08	0.12	0.09 ± 0.03
M4	0.10	0.11	0.11	0.07	0.09	0.08	0.12	0.10 ± 0.02
M5	0.13	0.12	0.12	0.09	0.10	*	0.14	0.12 ± 0.02
Prox. ROI Volume								
M1	1.42	1.35	1.46	0.74	1.10	1.09	1.70	1.27 ± 0.31
M2	0.44	0.74	0.72	0.55	0.54	0.65	0.83	0.64 ± 0.13
M3	0.54	0.69	0.65	0.38	0.59	0.56	0.74	0.59 ± 0.12
M4	0.54	0.49	0.66	0.37	0.51	0.46	0.67	0.53 ± 0.11
M5	0.65	0.48	0.69	0.54	0.54	*	0.79	0.62 ± 0.12
Dist. ROI								
M1/M2	2.610	2.588	2.309	2.269	2.319	2.709	2.099	2.42 ± 0.22
M1/M3	3.373	3.118	3.117	2.697	5.745	6.730	2.583	3.91 ± 1.64
M1/M4	2.913	3.270	3.067	3.122	2.555	3.242	3.264	3.06 ± 0.26
M1/M5	3.778	4.291	4.259	2.490	4.488	*	3.394	3.78 ± 0.75
Midl. ROI								
M1/M2	3.515	2.267	3.217	1.864	2.667	2.308	2.991	2.69 ± 0.59
M1/M3	2.762	2.156	3.141	2.196	2.627	2.169	2.629	2.53 ± 0.37
M1/M4	2.275	2.307	2.363	1.864	1.978	2.279	2.694	2.25 ± 0.27
M1/M5	1.799	2.248	2.244	1.337	1.853	*	2.296	1.96 ± 0.38
Prox. ROI								
M1/M2	3.210	1.831	2.035	1.344	2.043	1.676	2.062	2.03 ± 0.58
M1/M3	2.643	1.950	2.245	1.950	1.866	1.948	2.298	2.13 ± 0.28
M1/M4	2.619	2.780	2.214	1.992	2.138	2.351	2.542	2.38 ± 0.28
M1/M5	2.174	2.803	2.105	1.389	2.039	*	2.153	2.11 ± 0.45

Volume values are in cm^3. Each column gives values in order of foot ray. Ratios for each ROI correspond on ratio between first metatarsal volume and one of the lateral metatarsal volumes.
Abbreviations: Dist., distal; midl., midlength; prox., proximal.
*Not measurable.

between 0.29 cm^3 and 0.46 cm^3 for the lateral metatarsal bones. Each ROI volumes of M1 were always the most important. For lateral metatarsals, the most important distal ROI volume was always the second metatarsal. On midlength ROI, the mean volume was 0.22 ± 0.07 cm^3 (0.12; 0.33) for M1 and between 0.08 and 0.12 cm^3 for lateral metatarsals. On proximal ROI, the mean volume was 1.27 ± 0.31 cm^3 (0.74; 1.46) for M1 and between 0.53 cm^3 and 0.64 cm^3 for lateral metatarsals, without any specific distribution. The volume ratio, calculated between M1 and lateral metatarsal volumes (Table 4), was the smallest on distal ROI for M2 (mean 2.42, standard deviation ± 0.22) and the highest on midlength ROI (mean 2.69, standard deviation ± 0.59). According to cross-sectional surface, all metatarsal

TABLE 5 Cross-sectional area results at 3 levels of metatarsals

	Foot 1	Foot 2	Foot 3	Foot 4	Foot 5	Foot 6	Foot 7	Means
Dist. ROI CS area								
M1	2.51	2.51	2.88	1.54	2.26	2.68	2.97	2.48 ± 0.48
M2	0.96	0.97	1.25	0.68	0.97	0.99	1.42	1.03 ± 0.24
M3	0.75	0.81	0.92	0.57	0.39	0.40	1.15	0.71 ± 0.28
M4	0.86	0.77	0.94	0.49	0.88	0.83	0.91	0.81 ± 0.15
M5	0.67	0.59	0.68	0.62	0.50	*	0.88	0.65 ± 0.13
Midl. ROI CS area								
M1	1.16	1.32	1.34	0.62	0.88	0.90	1.63	1.12 ± 0.34
M2	0.33	0.58	0.42	0.33	0.33	0.39	0.55	0.42 ± 0.11
M3	0.42	0.61	0.43	0.28	0.34	0.42	0.62	0.44 ± 0.13
M4	0.51	0.57	0.57	0.33	0.45	0.40	0.61	0.49 ± 0.10
M5	0.65	0.59	0.60	0.46	0.48	*	0.71	0.58 ± 0.10
Prox. ROI CS area								
M1	3.56	3.38	3.65	1.86	2.75	2.73	4.26	3.17 ± 0.79
M2	1.11	1.85	1.79	1.38	1.35	1.63	2.07	1.60 ± 0.33
M3	1.35	1.73	1.63	0.95	1.47	1.40	1.85	1.48 ± 0.30
M4	1.36	1.63	1.65	0.93	1.29	1.16	1.68	1.33 ± 0.27
M5	1.64	1.73	1.73	1.34	1.35	*	1.98	1.54 ± 0.29

Area values are in cm^2. Each column gives values in order of foot ray (M1, first metatarsal; M2, second metatarsal; M3, third metatarsal; M4, fourth metatarsal; M5, fifth metatarsal). These values correspond to the first set of measurements.
Abbreviations: Dist., distal; midl., midlength; prox., proximal.
*Not measurable.

bones had their most important section on proximal extremity (Table 5). For M2, mean values showed the most important section for the proximal and the distal ROI (1.60 ± 0.33 cm^2 and 1.03 ± 0.24 cm^2, respectively), and the smallest section for the midlength ROI (0.42 ± 0.11 cm^2).

Statistical Analysis

The Shapiro-Wilk test showed that only the parameters of cross-sectional areas had a normal distribution ($P < .001$).

For the repeatability analysis, the ICCs were 0.99 for length and 0.63 for intrinsic torsion with manual measurement, and with CA techniques >0.99 for cross-sectional areas and 0.98 for intrinsic torsion.

Through the likelihood ratio test (19), we have underlined a significant difference between ICCs of both measurement techniques for intrinsic torsion ($P < .1E-12$). The reproductibility of the metatarsal intrinsic torsion measurement was better with the CA technique than with the manual technique (Table 6).

TABLE 6 Intraclass correlation coefficients

	Intraclass correlation coefficient (confidence interval 95%)
Length (manual measure)	0.99 (0.988–0.996)
Intrinsic torsion (manual measure)	0.61 (0.513–0.823)
Distal cross-sectional area (CA measure)	>0.99 (0.998–0.999)
Midlength cross-sectional area (CA measure)	>0.99 (0.9991–0.9997)
Proximal cross-sectional area (CA measure)	>0.99 (0.996–0.999)
Intrinsic torsion (CA measure)	0.98 (0.970–0.991)

Results of the ICC coefficent for the principal anatomic parameters show the difference in torsion measure between manual and CA techniques.

Discussion

The aim of this study was to first identify and then measure the intrinsic torsion of metatarsals. Another goal was to calculate metatarsal cross-sectional areas and evaluate our specific system of medical image analysis.

According to manual biometry data, our bone sets were unspecific. The limit of this first evaluation was clearly linked with the reliability of a direct reading technique. The variability of intrinsic torsion results by manual measurement was important (ICC, 0.61) against the CA measurement (ICC, 0.98). Direct reading techniques have been used exclusively for a long time and came from anthropometry techniques (20). They offer limited access to bone only through its external volume, and the cross-sectional area can only be approximated by direct linear measurement. On the contrary, CA techniques can give objective, 3-dimensional, and more reproducible measurements.

Principal axes of inertia are the first to build a geometric representation of the studied bone. It is simplified by considering bone tissue as an isotropic and homogeneous ma-

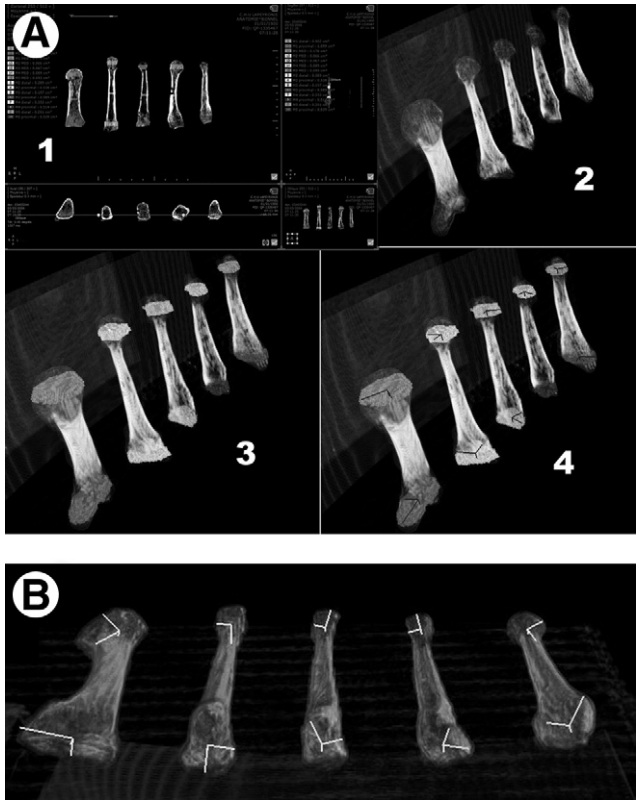

FIGURE 2 (*A*) ROI and inertial axis: MYRIAN analysis on a metatarsal set. For each set of bones (*2*), we defined the specific ROI with MYRIAN (*1*) and we obtained volume reconstruction (*3*) and axes of inertia (*4*). (*B*) ROI and inertial axis: visual result of MYRIAN process on a metatarsal set. For each specific ROI, we obtained the 3 inertial axes, and the most important was chosen to represent ROI principal axis.

terial. This approximation and cadaveric embalmed bones used as studied material exclude a densitometric approach for calculation of inertial parameters.

The CA study by inertial parameters for foot anatomy was first proposed by Udupa et al (10). Their functional evaluation of the hindfoot was performed with MRI and 3DVIEWNIX software (MPIG—University of Pennsylvania, Philadelphia, PA). Geometric data for foot characterization were formalized by Stindel et al (4). Several methods have been proposed to perform a functional study of the hindfoot skeleton (8, 9, 11). The dedicated software MYRIAN has allowed us to calculate some biometric parameters by using inertial criteria. These functionalities of inertial parameters are similar to 3DVIEWNIX as proposed by Udupa et al (3). The principal technical specificity in this study seems to be for segmentation. We chose a series of slices to characterize specific parts of each bone (ROI). Delineation on each slice was performed with a CA segmentation tool. Reconstruction of the 3-dimensional structure of each ROI on its 3-dimensional CT scan metatarsal view was performed by interpolation on each slice. We must emphasize that our

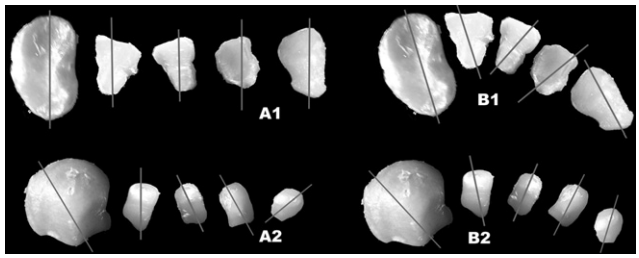

FIGURE 3 Intrinsic torsion and forefoot geometry. For metatarsal basis in axial layout (*A1*), cephalic extremities present anarchic positions (*A2*). For physiologic layout of the metatarsal basis (*B1*), we note a harmonious configuration of the metatarsal heads (*B2*).

work was performed on CT scan images from bones that were free of soft tissue. Technical possibilities of the bone segmentation tool in analysis software are more efficient in these conditions than for MRI in an in vivo study. By using medical imaging, CT scan or MRI, it is conceivable to use CA analysis on clinical evaluation as a preoperative surgical plan.

In our objective of precise characterization of the metatarsal intrinsic torsion, we were not able to use the midlength ROI to determine proximal and distal intrinsic torsions. This limit was associated with the chosen technical method. In fact, midlength cross-sectional surface of the lateral metatarsals is circular. This geometric form cannot be characterized by a single stable axis. For distal or proximal ROI, the general aspect of cross-sectional area was oval or piriformis. These forms are easy to characterize by a specific and stable axis.

Intrinsic torsion values proposed in this work showed the pronation angle for all metatarsals except for fifth ray, which was in supination. We have noted 3 patterns according to the pronation angular range. For M1, the intrinsic torsion was in large pronation with a great variability. For M3 and M4, we noted comparable values but with moderate variability. The torsion angle was smallest for M2. Axial rotation of metatarsal bones seems to be the outcome of rotational forces applied on the forefoot skeleton, and pronation stress appears to be the most important. The forces applied on M2 produce for essential dorsoplantar stresses (21). We assume that rotational forces on M2 are moderate or balanced between medial and lateral rotation. On M2, the geometric principal axes of proximal and distal ROI are at a global dorsoplantar direction.

The proximal ROI axis is important in torsion angle range. In this work, the physiologic positions of bones have not been noted according to tarsometatarsal joint reference. Nevertheless, a reconstruction of the natural proximal arch with views of the metatarsal basis (Figure 3) shows the variability in orientation of the proximal principal axes. Therefore, the intrinsic torsion can appear like an anatomic "correction" of the extrinsic rotation produced at the tarsometatar-

sal and more proximal joints. The metatarsal cephalic orientation, along with the anterior arch support, depends on this axial correction. In this functional relation, M2 was presented as the central axis of the anterior arch (22, 23), and the distribution of the metatarsals was in pronation for M1 and supination for M3, M4, and M5 (Figure 3). To our knowledge, no study about the extrinsic metatarsal rotation has been performed. Specific problems with weight load and difficulties with 3-dimensional images (MRI or CT scans) of the weight bearing foot are likely some of the limitations of this evaluation.

For M5, the intrinsic torsion was in supination. This is linked to the 3-dimensional conformation of the proximal extremity of M5. The fixation of the fibular brevis tendon gives a specific geometry to the M5 basis. But the axis of the articular surface is nearly at 90° of the basis of its principal axis. The result of supination for the M5 torsion angle is a consequence of the association between the technique that is used and the particular 3-dimensional structure of bone basis. The anterior support of the forefoot is not just dependent on metatarsal length or metatarsal slope. Intrinsic torsion appears important and specific in the anatomic characterization of the forefoot. Its evaluation and its correction could be a new approach in surgical procedures for metatarsalgia.

The volumes and cross-sectional area results for the midlength ROI are compatible with a study on cross-sectional anatomy of the human forefoot presented by Griffin and Richmond (18). With geometric parameters, they explained the weakness of the midlength part of M2 and M3. It contrasts with the significant stress these metatarsals take. This can be explained by the important capacity of plantar soft tissues in absorption of the mechanical energy during gait (24). Nevertheless, we have performed our approach on 3 parts: proximal, midlength, and distal. For the midlength ROI, we have noted the smallest volumes and cross-sectional areas for M2 and M3. No specific characteristic can be underlined for the proximal ROI of the lateral metatarsals. But for the distal ROI of M2, these parameters were the highest for the lateral metatarsal bones. After the distal extremity of M1, the M2 head is an essential point of mechanical strength. This relative distal strength opposes the midlength weakness. Mechanical characteristics of bone are not just summed up in cross-sectional geometric parameters. We could not evaluate bone density or histologic bone structure. But the distal extremity of M2 has a specific cross-sectional area that is combined with the smallest intrinsic metatarsal torsion. This geometric structure is the inference of mechanical stress (17, 25). In a study on plantar pressure during the push-off phase of gait, Hayafune et al (26) showed that the most important pressure increase is under the head of M2 for lateral metatarsals. The anatomy of M2, especially in its distal part, is suitable for this stress. Also, limited intrinsic torsion is suitable for dorsoplantar mechanical forces. At its basis, M2 presents no specific geometric parameter but a fitted fixation into the cuneiformis bones (27). All these considerations confirm that M2 must be considered the real axial rod of the forefoot.

In this study on geometric parameters of the forefoot skeleton, we have emphasized the intrinsic torsion of metatarsals. For us, this characteristic is an essential aspect in the anatomy of the forefoot for functional understanding or surgical approach. We have also presented an evaluation of the metatarsals' cross-sectional areas, which shows a specific distribution for the second metatarsal. The new technical systems offered us a better reliability in our measurements. This work will have to be completed with evaluations of the extrinsic torsions and the effective mobilities of the metatarsal bones in weightbearing conditions.

References

1. Schneider W, Knahr K. Metatarsophalangeal and intermetatarsal angle: different values and interpretation of postoperative results dependent on the technique of measurement. Foot Ankle Int 19:532–536, 1998.
2. Thomas J, Kunkel M, Lopez R, Sparks D. Radiographic values of the adult foot in standardized population. J Foot Ankle Surg 45:3–12, 2006.
3. Udupa JK, Odhner D, Samarasekera S, Goncalves RJ, Iyer K, Venugopal K, Furuie S. 3DVIEWNIX: an open, transportable, multidimensional, multiparameteric imaging software system. Proceedings of SPIE—The International Society for Optical Engineering 2164:58–73, 1994.
4. Stindel E, Udupa JK, Hirsch BE, Odhner D, Couture C. 3d MR image analysis of the morphology of the rear foot: application to classification of bones. Comput Med Imaging Graph 23:75–83, 1999.
5. Crisco JJ, McGovern RD, Wolfe SW. Noninvasive technique for measuring in vivo three dimensional carpal bone kinematics. J Orthop Res 17:96–100, 1999.
6. Canovas F, Roussanne Y, Captier G, Bonnel F. Study of carpal bone morphology and position in three dimensions by image analysis from computed tomography scan of the wrist. Surg Radiol Anat 26:186–190, 2004.
7. Canovas F, Prudhomme M, Jaeger M, Bonnel F. Three-dimensional reconstruction of the wrist and biometry of the carpal bones. Proceedings of the 3rd European Association of Clinical Anatomy Congress. Surg Radiol Anat, p abs 191, 1995.
8. Swider P, Scandella M, Baunin C, Cahuzac JP. Improvement of the 3D deformation diagnosis of infant clubfoot. 12th Conference of the European Society of Biomechanics, Dublin, 2000.
9. Cahuzac JP, Navascues J, Baunin C, Salles de Gauzy J, Estivalezes E, Swider P. Assessment of the position of the navicular by three-dimensional magnetic resonance imaging in infant foot deformities. J Pediatr Orthop B 11:134–138, 2002.
10. Udupa JK, Hirsch BE, Hillstrom HJ, Bauer GR, Kneeland JB. Analysis of in vivo 3-d internal kinematics of the joints of the foot. IEEE Trans Biomed Eng 45:1387–1396, 1998.
11. Mattingly B, Talwalkar V, Tylkowski C, Stevens D, Hardy P, Pienkowski D. Three-dimensional in vivo motion of adult hind foot bones. J Biomech 39:726–733, 2006.
12. Siegler S, Udupa JK, Ringle SI, Imhauser CW, Hirsch BE, Odhner D, Saha PK, Okereke E, Roach N. Mechanics of the ankle and subtalar joints revealed through a 3D quasi-static stress MRI technique. J Biomech 38:567–578, 2005.

13. Camacho D, Ledoux W, Rohr E, Sangeorzan B, Ching R. Three-dimensional, anatomically detailed foot model: a foundation for a finite element simulation and means of quantifying foot-bone position. J Rehabil Res Dev 39:401–410, 2002.
14. Jacob S, Patil KM, Brank LH, Huson A. Stresses in a 3D two arch model of a normal human foot. Mech Res Commun 23:387–393, 1996.
15. Cheung J, Zhang M, Leung A, Fan Y. Three-dimensional finite element analysis of the foot during standing—a material sensitivity study. J Biomech 38:1045–1054, 2005.
16. Chen WP, Tang FT, Ju CW. Stress distribution of the foot during mid-stance to push-off in barefoot gait: a 3-D finite element analysis. Clin Biomech 16:614–620, 2001.
17. Muehleman C, Bareither D, Manion BL. A densitometric analysis of the human first metatarsal bone. J Anat 195:191–197, 1999.
18. Griffin N, Richmond R. Cross-sectional geometry of the human forefoot. Bone 7:253–260, 2005.
19. Giraudeau B, Porcher R, Mary JY. Power calculation for the likelihood ratio-test when comparing two dependent intraclass correlation coefficients. Comput Methods Programs Biomed 77:165–173, 2005.
20. Volkov T. Variations squelettiques du pied chez les primates et dans les races humaines. PhD thesis. 1905. Faculté des Sciences, Paris, France.
21. Maestro M. Biomechanics of the forefoot. In *Chirurgie de l'avant-pied*, pp 23–38, edited by B Valtin and T Leemrijse, Elsevier SAS, Paris, 2005.
22. Hendrix G. Pathologie des déformations statiques des voûtes du pied. Bull Soc Belge Orthop 6:3, 1934.
23. De Doncker E, Kowalski C. Le pied normal et pathologique. Acta Orthop Belg 36:377–560, 1970.
24. Chi KJ, Schmitt D. Mechanical energy and effective foot mass during impact loading of walking and running. J Biomech 38:1387–1395, 2005.
25. Perry JE, Ulbrecht JS, Derr JA, Cavanagh PR. The use of running shoes to reduce plantar pressures in patients who have diabetes. J Bone Joint Surg (Am) 77:1819–1828, 1995.
26. Hayafune N, Hayafune Y, Jacob H. Pressure and force distribution characteristics under the normal foot during the push-off phase in gait. Foot 9:88–92, 1999.
27. Bojsen-Møller F. Anatomy of the forefoot, normal and pathologic. Clin Orthop 142:10–18, 1979.